Enhancement of semiconducting single-wall carbon nanotubes photoluminescence

Etienne Gaufrès[1], Nicolas Izard[2+], Laurent Vivien[1*], Saïd Kazaoui[2], Delphine Marris-Morini[1] and Eric Cassan[1]

1: Institut d'Electronique Fondamentale, CNRS-UMR 8622, Université Paris-Sud 11, 91405 Orsay, France

2: National Institute of Advanced Industrial Science and Technology (AIST), 1-1-1 Higashi, Tsukuba, Ibaraki 305-8565, Japan

+: Currently at Institut d'Electronique Fondamentale

laurent.vivien@u-psud.fr

Photoluminescence properties of semiconducting single wall carbon nanotubes (s-SWNT) thin films with different metallic single wall carbon nanotubes (m-SWNT) concentrations are reported. s-SWNT purified samples are obtained by polymer assisted selective extraction. We show that a few m-SWNT in the sample generates a drastic quenching of the emission. Therefore, highly purified s-SWNT films are a strongly luminescent material and a good candidate for future applications in photonics, such as near infrared emitters, modulators and detectors. © 2010 Optical Society of America

OCIS codes: 160.2540, 160.4236, 160.4760, 260.2510, 300.6280

Single wall carbon nanotube (SWNT) is a unique monodimensional material, exhibiting unusual electronic and optical properties, making it an ideal candidate for future optoelectronic [1] and all-optical devices [2]. The nanotube structure, defined by the so-called (n,m) chiral index, fixes all the nanotubes properties, such as metallic or semiconducting behavior. Semiconducting nanotubes (s-SWNT) are of particular interest in photonics for their direct band-gap, allowing near-IR luminescence (PL) from electron-hole recombination. In the last few years, numerous impressive results have been obtained on the photoluminescence properties of SWNT, where luminescence arise from well-isolated s-SWNT, either in solution by wrapping with surfactant [3–5], or dispersion in gelatin matrix [6, 7]. Recently, photoluminescent composite gels have also been demonstrated [8]. Indeed, s-SWNT are extremely sensitive to their environment. An incomplete isolation, resulting in small bundles

1

or metallic nanotubes (m-SWNT) in contact with s-SWNT, will lead to the creation of alternative non-radiative de-excitation paths and ultimately an effective quenching of the photoluminescence. It has been estimated that only around 10 % of the s-SWNT embedded in gelatin matrix effectively participate in the fluorescence, the remainder being quenched by left-over m-SWNT, bundles or impurities [7]. The direct influence of m-SWNT removal on the nanotubes optical properties was never really studied. Several approaches have been explored in the past few years for optimizing the diameter and chirality selection of SWNTs, such as chemical functionalization, DNA, polymer wrapping and density gradient centrifugation techniques [9–14]. The possibility to achieve chiral specific SWNT extraction is indeed very promising for future photonic applications. Recently, we demonstrated that the use of poly-9,9-di-n-octyl-fluorenyl-2,7-diyl (PFO) in toluene as an extracting agent followed by ultracentrifugation allows to obtain quasi metallic-free SWNT [15]. Using sample with a constant concentration in s-SWNT but differents concentrations in m-SWNT, we show in this paper that the presence of even a few metallic nanotubes quenche the strong intrinsic photoluminescence properties of s-SWNT.

Samples were prepared as previously described [15]. First, SWNT powder (as-prepared HiPco, Carbon Nanotechnologies Inc.), poly-9,9-di-n-octyl-fluorenyl-2,7-diyl (PFO) (Sigma-Aldrich) and toluene were mixed in the ratio of SWNT (5mg):PFO (20mg):toluene (30ml) and homogenized by sonication (for 1 h using a water-bath sonicator and 15 min using a tip sonicator). Then this mixture was centrifugated for 5-60 min using either a desktop centrifuge (angle rotor type, 10.000g) or an ultracentrifuge (swing rotor type, 150.000g), after which the upper 80 % of the supernatant solution was collected. We shall focus on two types of SWNT solution: solution centrifugated at 10.000g for 15 min (labeled L) and solution centrifugated at 150.000 g for 2 hours (labeled S). We also consider the non centrifugated solution (labeled R) for comparison purpose. At this stage, the concentration of solutions R and L were adjusted by dilution to match the most intense absorption peak around 1200 nm (1.03 eV) of sample S to assure the same amount of s-SWNTs in all off the solutions (cf. Figure 1a). Solutions were then spin coated several times onto glass substrate at 500 RPM for 60 s to achieve a layer thickness around 200 nm [16]. Lastly, samples were annealed at 150 ^{o}C for 15 min.

Absorption spectra of R, L and S samples in toluene are presented in Figure 1a. Sharp peaks in the range of 1050-1400 nm (1.18-0.89 eV, labeled E_{11}) and 600-900 nm (2.07-1.38 eV, E_{22}) are the optical absorption bands corresponding respectively to the first and second transitions between Van Hove singularities in the s-SWNT density of states. Peaks in the range of 500-600 nm (2.48-2.07 eV, M_{11}) correspond to the absorption bands of m-SWNTs [17]. Peak intensities gradually diminished and eventually vanished when all the m-SWNTs were removed by ultracentrifugation in sample S. The absorption background also

2

drastically reduced after the first low gravity (G) centrifugation. Indeed, the centrifugation step permits the effective removal of amorphous carbon and catalyst impurities initially present in the HiPCO SWNT powder. Raman spectra for samples L and S were recorded at 514.5 nm (2.41 eV) and the radial breathing mode (RBM) and tangential mode (TM) regions are reported in Figure 1 b and c, respectively. Raman spectroscopy is a resonant process for SWNT, and the RBM peak at 190 cm^{-1} is specific to s-SWNT while the RBM peak at 270 cm^{-1} is specific to m-SWNT [18]. We observed that m-SWNT peaks present in sample L completely vanished in sample S. This is coherent with the TM regions, where the broad asymmetric line shape between 1400 and 1600 cm^{-1} of sample L, characteristic of a metallic behavior, completely disappears in sample S. Further electric measurements presented in reference [15] confirm the absence of m-SWNT in sample S. According to absorption and Raman measurements, the first low G centrifugation step (sample L) effectively remove the initially present amorphous carbon and catalyst impurities, but also remove some m-SWNT. The high G centriguration step (sample S) remove all the remaining m-SWNT. Thus, the composition of samples L and S differ only by the presence of m-SWNT in sample L.

The PL excitation-emission maps of each samples were obtained using a Titane Sapphire (Ti:Sa) laser pumped by a cw Ar laser. Ti:Sa laser delivers continuous light at a wavelength range from 700 nm to 840 nm (1.77 to 1.48 eV). Photoluminescence signal is then recorded at room temperature using a monochromator (JobinYvon 550) coupled with a cooled InGaAs detector with a 3 nm step. Emission intensity as a function of both excitation (from 700 to 840 nm / 1.77 to 1.48 eV) and emission wavelength (from 1000 to 1600 nm / 1.24 to 0.78 eV) was recorded. The experimental values were corrected by taking into account the system response. Results are presented in Figure 2a, b and c, each map being normalized by the maximal intensity. Figure 2d shows the chirality map for the photoluminescent nanotubes from raw nanotubes in sample R and PFO purified s-SWNT in sample S. We discovered, as previously observed by Chen et al. [13], a chiral selectivity of PFO polymer. Indeed, chirality in the starting material were evenly distributed inside the measuring range, with chiral angle ranging from 3.96° in (12,1) tube to 27.8° in (8,7) tubes. In contrast, PFO-extracted nanotubes consist of only two tubes in the measuring range, 73 % of (8,6) and 27 % of (8,7) nanotubes [19]. Those two nanotubes possess near armchair structure with high chiral angles above 25°. The exact mechanism of PFO's high chiral selectivity is still unknown, but the aromatic structure of the polymer may play a major role in the wrapping interaction with nanotubes [14].

In order to determine the influence of the purification process, SWNT photoluminescence intensity for an excitation energy of 1.7 eV is displayed in Figure 3. Particular care was given to obtain the three samples with roughly the same concentration of (8,6) s-SWNT as shown on Figure 1a, which permit a comparison of the photoluminescence intensity level. Further-

3

more, photoluminescence intensity of S and L samples were corrected by the absorption peak intensity at 1.7 eV after background substraction. It was not possible to properly remove all background contribution in R sample; uncorrected photoluminescence intensities of all three samples are presented in the inset of Figure 3. The most striking feature is the impressive increase of (8,6) nanotube photoluminescence intensity with the degree of purification. Indeed, while sample R presents a rather low signal, samples L and S exhibit PL signal enhancement. An increase by a factor of 3 is observed in the PL intensity of (8,6) nanotube for sample S as compared to L. PL intensities of L and S samples increase by a factor of 2 and 6 respectively compared to sample R (unpurified). An analog increase was also observed for the intensity of the (8,7) nanotube, but as the relative concentration in (8,7) nanotube change between samples, the comparison is not as straightforward. It is remarkable that even if the concentration of (8,7) tube is higher in the starting material, the photoluminescence intensity is still 3 times higher in the PFO selectively extracted material. As the number of quenching centers constituted by m-SWNT decreases, most of the exciton recombination occurring in the (8,6) nanotubes likely contribute to the luminescence phenomenon, leading to an intensity increase of S sample by factor of 3 and 6 as compared to L and R samples, respectively.

In conclusion, we have studied the photoluminescence of pure semiconducting SWNT thin films, extracted by the PFO centrifugation technique. We found that the removal of m-SWNTs leads to an enhancement of the photoluminescence properties. Indeed, after removal of m-SWNT, the same quantity of (8,6) s-SWNT displays a 6-fold increase in photoluminescence intensity. The use of PFO as a matrix leads to the formation of well isolated nanotube thin films. These results are of major importance for the future use of s-SWNT thin film matrix in photonic applications.

References

1. P. Avouris, M. Freitag and V. Perebeinos, *Carbon-nanotube photonics and optoelectronics*, Nature Photonics **2**, 341 (2008)
2. S. Yamashita, Y. Inoue, S. Maruyama, Y. Murakami, H. Yaguchi, M. Jablonski, S.Y. Set, *Saturable absorbers incorporating carbon nanotubes directly synthesized onto substrates and fibers and their application to mode-locked fiber lasers*, Optics Letters **29**, 1581 (2004)
3. M.J. O'Connel, S.M. Bachilo, C.B. Huffman, V.C. Moore, M.S. Strano, E.H. Haroz, K.L. Rialon, P.J. Boul, W.H. Noon, C. Kittrell, J. Ma, R.H. Hauge, R.B. Weisman and R.E. Smalley, *Band Gap Fluorescence from Individual Single-Walled Carbon Nanotubes*, Science **297**, 593 (2002)
4. S.M. Bachilo, M.S. Strano, C. Kittrel, R.H. Hauge, R.E. Smalley and R.B. Weisman,

Structure-Assigned Optical Spectra of Single-Walled Carbon Nanotubes, Science **298**, 2361 (2002)

5. M.S. Arnold, J.E. Sharping, S.I. Stupp, P. Kumar and M.C. Hersam, *Band Gap Photobleaching in Isolated Single-Walled Carbon Nanotubes*, Nano Lett. **3**, 1549 (2003)

6. F. Wang, G. Dukovic, L.E. Brus and T.F. Heinz, *The Optical Resonances in Carbon Nanotubes Arise from Excitons*, Science **308**. 838 (2005)

7. S. Berger, C. Voisin, G. Cassabois, G. Delalande and P. Roussignol, *Temperature Dependence of Exciton Recombination in Semiconducting Single-Wall Carbon Nanotubes*, Nano Lett. **7**, 398 (2007)

8. C. Zamora-Ledezma, L. Anez, J. Primera, P. Silva, S. Etienne-Calas and E. Anglaret, *Photoluminescent single wall carbon nanotubesilica composite gels*, Carbon **46**, 1253 (2008)

9. C. Ménard-Moyon, N. Izard, E. Doris and C. Mioskowski, *Separation of Semiconducting from Metallic Carbon Nanotubes by Selective Functionalization with Azomethine Ylides*, J. Am. Chem. Soc. **128**, 6552 (2006)

10. L. Zhang, S. Zaric, X. Tu, X. Wang, W. Zhao and H. Dai, *Assessment of Chemically Separated Carbon Nanotubes for Nanoelectronics*, J. Am. Chem. Soc. **130**, 2686 (2008)

11. M.S. Arnold, A.A. Green, J.F. Hulvat, S.I. Stupp and M.C. Hersam, *Sorting carbon nanotubes by electronic structure using density differentiation*, Nature Nanotech. **1**, 60 (2006)

12. A. Nish, J.-Y. Hwang, J. Doig and R.J. Nicholas, *Highly selective dispersion of single-walled carbon nanotubes using aromatic polymers*, Nature Nanotech. **2**, 640 (2007)

13. F. Chen, B. Wang, Y. Chen and L.-J. Li, *Toward the Extraction of Single Species of Single-Walled Carbon Nanotubes Using Fluorene-Based Polymers*, Nano Lett. **7**, 3013 (2007)

14. J.-Y. Hwang, A. Nish, J. Doig, S. Douven, C.-W. Chen, L.-C. Chen and R.J. Nicholas, *Polymer Structure and Solvent Effects on the Selective Dispersion of Single-Walled Carbon Nanotubes*, J. Am. Chem. Soc. **130**, 3543 (2008)

15. N. Izard, S. Kazaoui, K. Hata, T. Okazaki, T. Saito, S. Iijima and N. Minami, *Semiconductor-enriched single wall carbon nanotube networks applied to field effect transistors*, Appl. Phys. Lett. **92**, 243112 (2008)

16. Layer thickness was estimated from ellipsometry spectroscopy and direct profilometer measurement.

17. I.W. Chiang, B.E. Brinson, A.Y. Huang, P.A. Willis, M.J. Bronikowski, J.L. Margrave, R.E. Smalley and R.H. Hauge, *Purification and Characterization of Single-Wall Carbon Nanotubes (SWNTs) Obtained from the Gas-Phase Decomposition of CO (HiPco Process)*, J. Phys. Chem. B **105**, 8297 (2001)

18. J.-L. Sauvajol, E. Anglaret, S. Rols and L. Alvarez, *Phonons in single wall carbon nanotube bundles*, Carbon **40**, 1697 (2002)
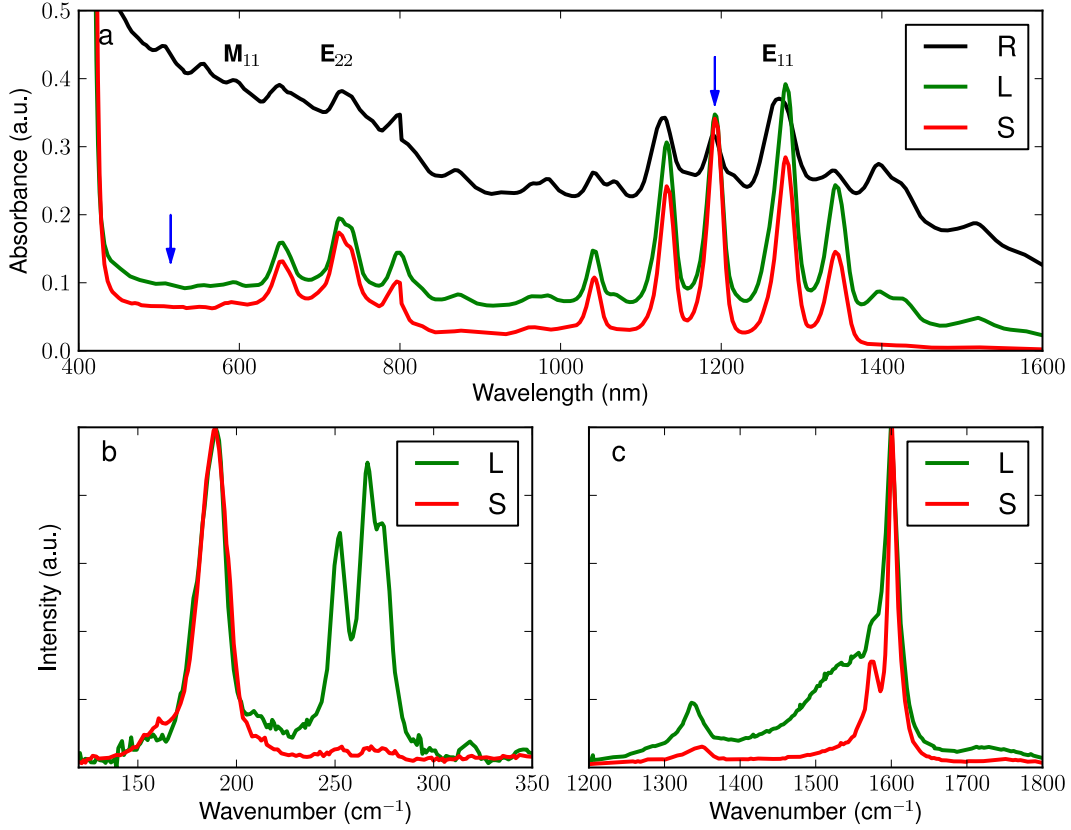
19. Determined using method described in Ref. [13]

Fig. 1. (color online) (a) The optical absorption spectra in toluene, (b) and (c) the RBM and TM Raman spectra at 2.41 eV of R, L and S samples. Arrows indicates respectively position of the Raman laser probe (left) and where the concentration adjustment was performed (right).
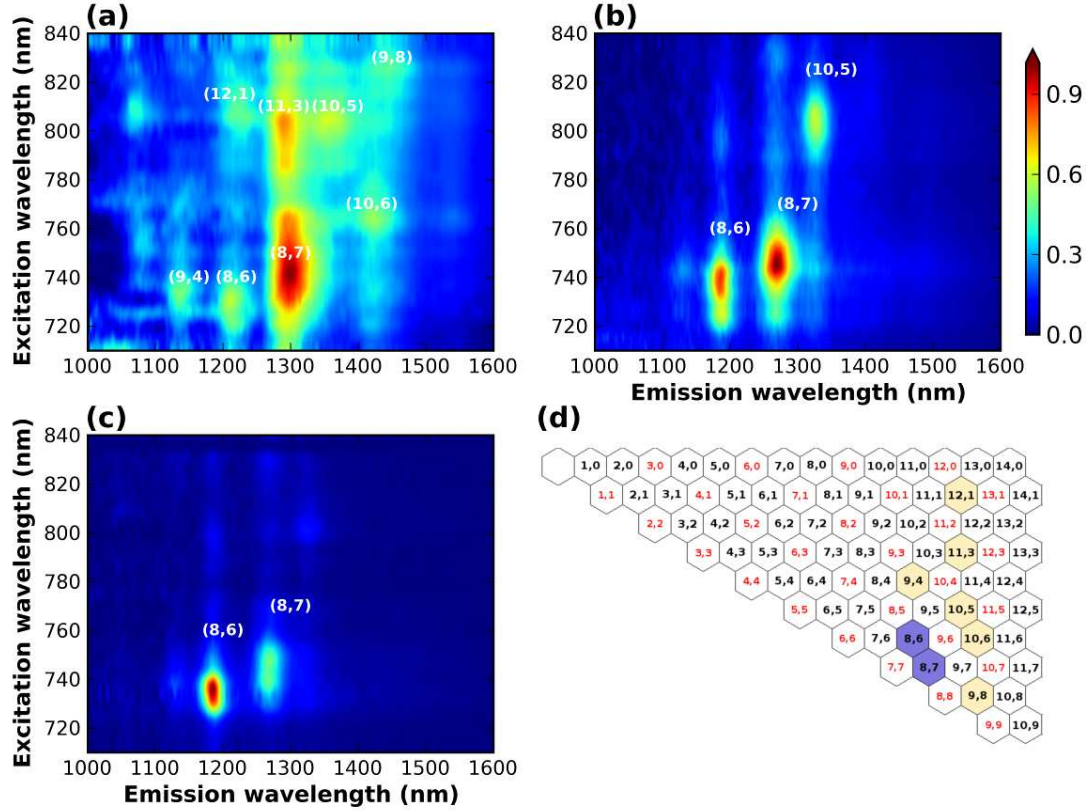
Fig. 2. (color online) Photoluminescence map (emission wavelength vs excitation wavelength) of PFO- embedded SWNT thin film spin-coated onto glass substrate. The layer thickness is around 200 nm. (a) Sample R, (b) sample L and (c) sample S. (d) Chiral map showing the wrapping preference of PFO (in blue / dark gray) as compared to raw HiPCO SWNT sample (in yellow / light gray).
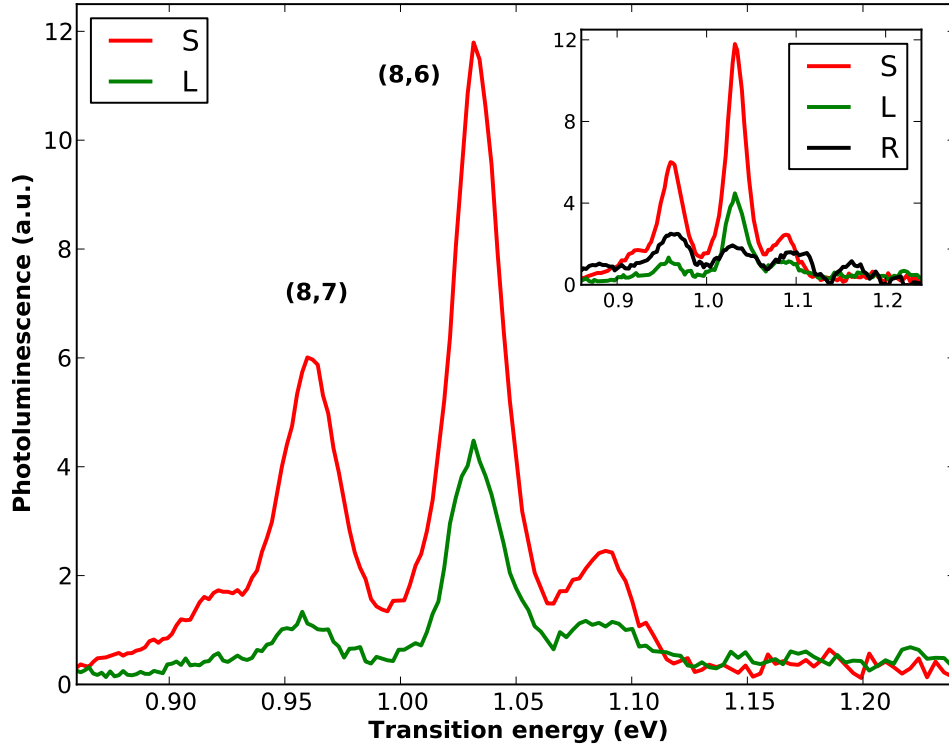
Fig. 3. (color online) Photoluminescence intensities of samples L and S which differ in m-SWNT concentration. Intensity was normalized taking into account the net intensity of light absorbed in s-SWNT at the pumping enegy (1.7eV). Inset: Photoluminescence intensities of L and S samples compared to R sample, without normalization.